Model documentation of:

How does nitrogen control soil organic matter turnover and composition? – Theory and model

Chun Chung Yeung[1], Harald Bugmann[1], Frank Hagedorn[2], Margaux Moreno Duborgel[2], Olalla Díaz-Yáñez[1]

[1]Forest Ecology, Institute of Terrestrial Ecosystems, Department of Environmental Systems Science, ETH Zurich, 8092 Zurich, Switzerland

[2]Forest Soils and Biogeochemistry, Swiss Federal Institute for Forest, Snow and Landscape Research (WSL), Birmensdorf, Switzerland

Table of Contents

Model Introduction

This document describes the soil model used in this study. The model formulations are based primarily on CENTURY v4.6 (Parton et al., 1987, Stergiadi et al., 2016) and model parameterization are based on ForCent, the forest version of CENTURY (Parton et al., 2010). We used the C and N cycles only and took the minimal functional part of CENTURY SOM model – litter partitioning and decomposition modules. The former partitions raw litter inputs into metabolic and structural litter, and the latter calculates the decomposition of all organic matter pools: metabolic (MetabC) and structural litter (StrucC), coarse deadwood (Wood1C), SOC1, SOC2 & SOC3. All C pools except SOC3 are situated in two layers (surface and top 20cm mineral soil layer). Decomposition leads to the emission of CO_2 and a flow of carbon (C) and nitrogen (N) between donor and receiver OM pools, as well as an exchange of N with the inorganic mineral N pool. The soil model takes in litter and soil water inputs estimated by ForClim v4.0.1, a stand-scale model of forest dynamics (Huber et al., 2020).

Figure S5 shows a schematic of the soil model, along with boundary inputs:

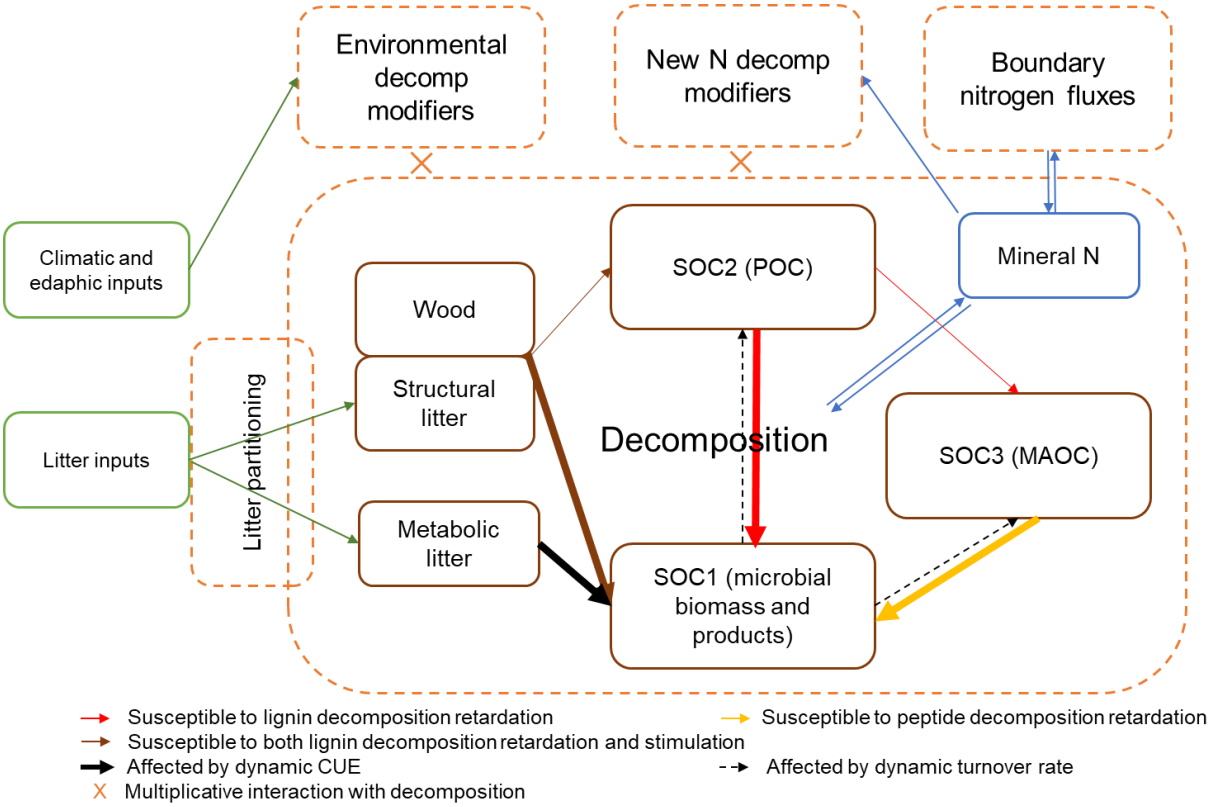

Figure S5: The overall model of this study, its inputs, state variables and processes. Brown solid boxes indicate the state variables in the SOM model updated monthly. All state variables (pools) exist in both the surface and mineral soil layers (0-20 cm), except for SOC3, which only exists in the mineral soil. Green boxes represent inputs to drive the model. Dashed boxes contain soil processes that run at a monthly time step. SOC1, SOC2 and SOC3 denote the carbon of fast-turnover, intermediate-turnover and slow-turnover SOM, respectively.

In the following equations, all variables except those with the "k" prefix, which denotes model parameters, are dynamic variables evolving through discrete time (Hence, we omitted a "t" subscript hereafter for simplicity). Variables starting with "g" are local variables updating every time it is re-calculated; those starting with "u" is either an input (from the plant or weather models) or an output variable of the soil model. Variables without any prefixes are state variables updated every month.

The SOM decomposition model is a first-order model (with respect to substrate amount) that runs at monthly timestep:

$$\frac{dC_x}{dt} = I - gTcflow_x \qquad (S1)$$

$$gTcflow_x = C_x \times kDec_x \times uDF_x \qquad (S2)$$

where C_x is a state variable carbon pool x at the current timestep t, I is the C input into C_x at time t, $gTcflow_x$ is the total amount of C flowing out of C_x at time t (bound below C pool size), $kDec_x$ is the monthly maximum turnover rate parameter of C_x and uDF_x is the environmental decomposition modifier associated with C_x at time t (the calculation of the decomposition modifiers are provided in the Section "*Overall decomposition modifier*").

Litter Production

Carbon input I ultimately comes from litter. We used ForClim v4.0.1, model variant 12 (Huber et al., 2020) to calculate annual litter (foliage, twig, root, exudates, wood) at the cohort level (a group of trees of the same age and species). For further details, please refer to Bugmann (1994).

The litter inputs of each kind of litter: Foliage, fine root, exudate, fine twig, above- and below-ground coarse deadwood are summed at the patch level (800m^2) and converted to per hectare values (i.e., each patch has multiple cohorts of the same kind of litter that can be summed). Furthermore, the annual litter (kg/ha/y) is converted to monthly litter (g/m^2/month) before entering the soil model by dividing with 12, with the exception of 1) deadwood (uWL) is added once to the soil at the beginning of each year and 2) deciduous foliage litter is added on October and November.

Foliage litter

The foliage litter of three litter quality classes (kLQ) is computed annually per cohort following this equation:

$$uFL_{c,kLQ} = gFolW_{c,kLQ} \times \left(\frac{Trs_c}{kFRT_s} + DTrs_c\right) \times kCDF \qquad (S3)$$

where $uFL_{c,kLQ}$ is the foliage litter (kg) produced annually by the current cohort c and for a specific kLQ class indicating litter quality (i.e., litter C:N ratio and lignin content), which is a species-specific parameter as defined in Bugmann (1994). $gFolW_{c,kLQ}$ is the simulated foliage mass (kg) in the current cohort and kLQ class, Trs_c and

$DTrs_c$ are the number of live and dead trees of the cohort respectively, $kFRT_s$ (year) is a species parameter representing foliage retention time of live trees, $kCDF$ is the carbon fraction of vegetative biomass.

Twig litter

Cohort twig litter is calculated annually by equation S4:

$$uTL_c = \frac{\pi}{4} \times {D_c}^2 \times kConv \times (Trs_c + DTrs_c) \times kCDF \qquad (S4)$$

where uTL_c is the annual twig litter (kg) produced by cohort c, D_c is the diameter at breast height (cm) of the current cohort c, $kConv$ is an empirical conversion factor between basal area (cm^2) and the amount of twigs litter (Bugmann, 1994). There is no litter quality class for twig.

Fine root litter

Cohort fine root litter is calculated annually by equation S5:

$$uRL_c = uFL_{c,kLQ} \times kRSR \qquad (S5)$$

where uRL_c is the annual fine root litter (kg) produced by cohort c, $kRSR$ is an empirical parameter for fine root litter (20cm depth) to foliage litter ratio (Appendix 2). There is no litter quality class for fine root.

Root exudate

Cohort root exudate is calculated annually by equation S6:

$$uEX_c = uRL_c \times kRER \qquad (S6)$$

where uEX_c is the annual root exudates (kg) produced by cohort c, $kRER$ is an empirical parameter for root exudate to fine root litter ratio. There is no litter quality class for root exudate.

Woody litter (coarse deadwood)

Cohort aboveground coarse woody litter (three litter quality classes) is calculated annually by equation S7:

$$uWL_{c,kLQ} = \left(gSBio_{c,kLQ} + gSBioWE_{c,kLQ}\right) \times DTrs_c \times kCDF \qquad (S7)$$

where $uWL_{c,kLQ}$ is the coarse deadwood litter (stemwood + large branches) produced annually (kg) by the current cohort c and for a specific kLQ class indicating litter quality (i.e., litter C:N ratio and lignin content), the same as in foliage litter. $gSBio_{c,kLQ}$ and $gSBioWE_{c,kLQ}$ are the estimated aboveground stem wood biomass (kg) and branch biomass (kg) respectively in the current cohort c.

Belowground dead coarse root is assumed to be 20% of $uWL_{c,kLQ}$ (He et al., 2018; Kurz et al., 1996).

Foliage litter and deadwood are classified under different litter quality classes kLQ depending on the tree species because leaf and wood are stoichiometrically correlated and functionally differed among species (Pietsch et al., 2014), whereas the other types of litter have relatively more similar quality across species (Liang et al., 2018).

Litter Partitioning

The fresh litter produced is converted to metabolic and structural litter as in CENTURY except for deadwood and root exudates. Deadwood has its own state variable pool (Wood1C) and does not go through litter partitioning. Root exudates go to metabolic litter directly (Berardi et al., 2024). Other types of litter are characterized by their C:N and lignin content, which are then converted to Lignin:N ratio used to calculate the fraction of litter partitioned into labile metabolic and recalcitrant structural litter:

$$gFrMet = kSpl_1 - kSpl_2 \times \left(\frac{frLig}{frN}\right) \qquad (S8)$$

where $gFrMet$ is the fraction of litter C being partitioned into metabolic litter, $frLig$ is the mass fraction of lignin in the original litter and frN is the mass fraction of total N in the original litter. $kSpl_1$ is the maximum fraction going into metabolic litter and $kSpl_2$ is a linear parameter relating lignin:N ratio to $frMet$. The fraction of litter C partitioned to structural litter is simply $1 - gFrMet$.

Litter N partitioning is based on the fixed C:N ratio of structural litter (kCNs) as a fixed model parameter i.e., the remainders of N go to metabolic litter.

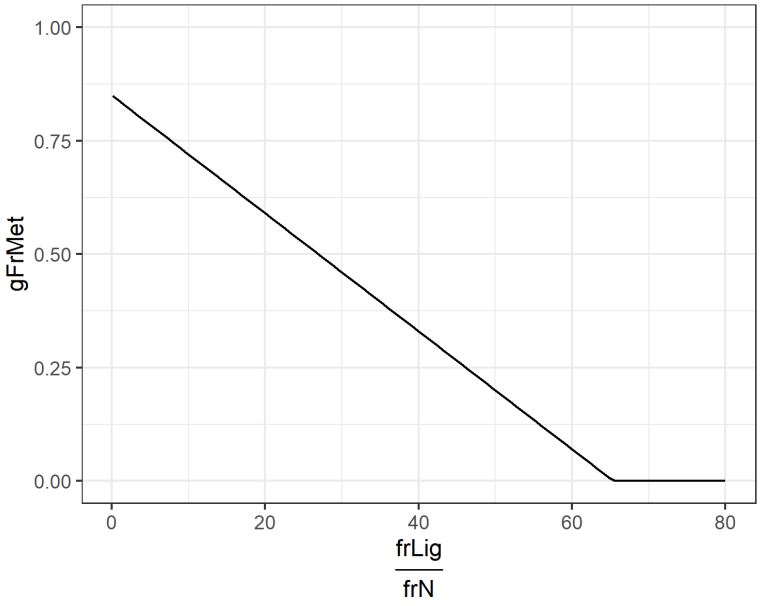

Figure S6: Fraction of litter C partitioned into metabolic litter (gFrMet) as a function of the ratio between the mass fraction of lignin (frLig) and the mass fraction of total N (frN) in the original litter.

Decomposition

Environmental decomposition modifiers

The environmental decomposition modifiers are a set of monthly scalars that reduce decomposition rate at sub optimal conditions, based on climatic or edaphic factors. Individual environmental modifiers based on soil temperature, moisture, anaerobic effect, soil pH and soil texture are later combined multiplicatively to give overall decomposition modifiers to reduce the decomposition rate of each C pool. All environmental modifiers range between 0 and 1 with the exception of temperature decomposition modifier below which could go slightly above 1.

Temperature

Our model uses a variable Q10 function inherited from CENTURY with low Q10 values at high temperatures and high Q10 values at low temperatures as defined in equation S9 (Del Grosso et al. 2005):

$$uDFtemp_m = \frac{\left(kTeff_2 + \left(\frac{kTeff_3}{\pi}\right) \times \operatorname{atan}\left(\pi \times kTeff_4 \times (uT_m - kTeff_1)\right)\right)}{gNormalizer} \qquad (S9)$$

where $uDFtemp_m$ is the temperature decomposition modifier calculated monthly, in the form of a sigmoidal function with four shape parameters $kTeff_1$, $kTeff_2$, $kTeff_3$, $kTeff_4$; uT_m is the monthly soil temperature (°C) at which the decomposition takes place (topsoil temperature is assumed to be equivalent to air temperature in the current model); and $gNormalizer$ is the temperature decomposition modifier at the reference soil temperature of 30°C calculated as:

$$gNormalizer = kTeff_2 + \left(\frac{kTeff_3}{\pi}\right) \times \operatorname{atan}\left(\pi \times kTeff_4 \times (30 - kTeff_1)\right) \qquad (S10)$$

Moisture

Soil moisture controls decomposition in a multifaceted manner by contributing to hydrolysis directly and serving as a medium for the transport of substrates and oxygen. The relationship of soil moisture content with decomposition is usually a negative-skewed unimodal curve, with the highest decomposition rate occurring just below field capacity and decreasing sharply above and below field capacity (Moyano et al., 2013; Sato & Seto, 1999; Schaufler et al., 2010; Zhang et al., 2013). In our soil model, this complex relationship is modeled by two separate effects: soil moisture decomposition modifier $uDFwater$ and anaerobic decomposition modifier $uDFan$ inherited from CENTURY (Berardi et al., 2024):

$$uDFwater_m = \frac{1}{(1 + kWeff_1 \times e^{(kWeff_2 \times uRWC_m)})} \qquad (S11)$$

where uDF_{water} is a logistic function, with shape parameters $kWeff_1$ and $kWeff_2$, and the input variable $uRWC_m$ (range 0-1) is the relative soil water content (relative to full available water capacity) calculated as follow:

$$uRWC_m = \frac{uSM_m}{kBS} \qquad (S12)$$

where uSM_m is the amount of soil moisture (cm) at the current monthly timestep, kBS is the available water capacity (cm) of the given soil. The soil water module is a simple water bucket model described in Bugmann (1994).

Anaerobic effect

In eq. (S11), uDF_{water} increases to 1 at the highest relative water content but in reality, decomposition slows down due to the onset of anaerobic conditions under water-logging. Hence an anaerobic effect is required and implemented as followed based on the ratio of soil water supply to potential evapotranspiration:

$$uDFan_m = \begin{cases} 1 & \text{if } (uRPRPET_m < kANeff_1) \\ 1 + kSlope \times \left((uRPRPET_m - kANeff_1) \times (1 - kDrain)\right) & \text{if } (kANeff_1 < uRPRPET_m < kANeff_2) \\ kANeff3 & \text{if } (uRPRPET_m > kANeff_2) \end{cases} \qquad (S13)$$

Where $uDFan_m$ is the anaerobic decomposition modifier, $uRPRPET_m$ is the ratio of monthly total soil water input including precipitation and snow melt (cm) to potential evapotranspiration (cm). $kANeff_1$ is the $uRPRPET_m$ below which there is no effect of soil anaerobic conditions on decomposition, $kANeff_2$ is the $uRPRPET_m$ above which there is maximum impact of soil anaerobic conditions on decomposition, and $kANeff3$ is the maximum anaerobic effect (lowest value). $kSlope$ is the linear slope parameter calculated by the combination of these base parameters following eq. (S14) below. The parameter $kDrain$ (range 0-1) is a user defined parameter representing whether the soil is poor-drained or well-drained and dampens the anaerobic effect in well-drained soils, We equated it to sand fraction in this study.

$$kSlope = (1 - kANeff_3)/(kANeff_1 - kANeff_2)) \qquad (S14)$$

Soil pH

The soil pH decomposition modifier $uDFpH$ has the same sigmoid function as uDF_{temp} (eq. (S9)) as it is based on the same assumption that beyond a certain optimal pH, decomposition rate will plateau (pH >= 7), but below the optimal pH (i.e. acidic conditions), decomposition is reduced.

$$uDFpH = kPHeff_2 + \left(\frac{kPHeff_3}{\pi}\right) \times \text{atan}\left(\pi \times kPHeff_4 \times (kpH - kPHeff_1)\right) \qquad (S15)$$

Where $uDFpH$ is the soil pH decomposition modifier (Fig. S7) with 4 shape parameters $kPHeff_1$, $kPHeff_2$, $kPHeff_3$, $kPHeff_4$, kpH is the average pH of the soil profile. Note that $kPHeff_1$ is a parameter representing the pH sensitivity of the decomposer and assumes a different value for each C pool according to CENTURY (see Appendix 2).

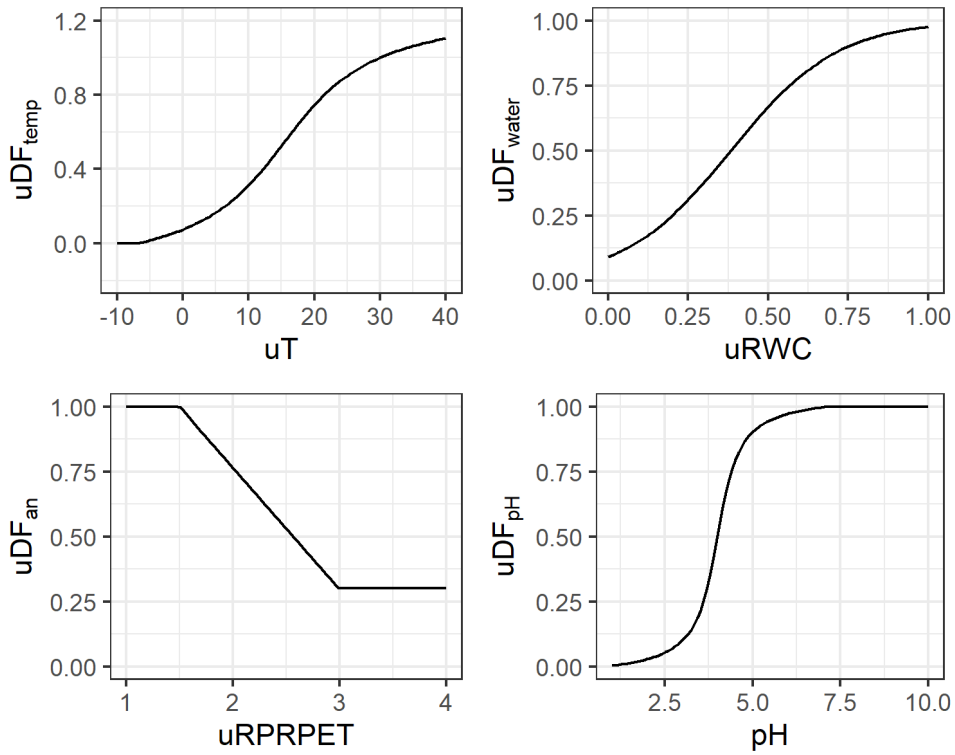

Figure S7: Decomposition modifier uDFtemp, uDFwater, uDFan, uDFpH as a function of environmental conditions: air temperature (uT), relative water content (uRWC), ratio of precipitation to potential evapotranspiration (uRPRPET) and soil pH (relative to $kPHeff_1 = 4$), respectively.

Soil texture

The soil texture effect modifier on decomposition (only affects soil SOC1) is calculated following eq. (S16):

$$uDFsand = kSeff_1 + kSeff_2 \times kSand \qquad (S16)$$

where $uDFsand_m$ is a linear function of sand fraction $kSand$, $kSeff_1$ is the effect at zero sand content and $kSeff_2$ is the linear slope parameter.

Overall decomposition modifier

Depending on the carbon pool (metabolic and structural litter, wood, SOM1, SOM2 and SOM3) and the soil layer concerned (surface or mineral soil), different climatic and edaphic decomposition modifiers are multiplied together as one overall decomposition modifier to reduce decomposition rate. For the overall decomposition modifier of C pools in the surface layer, eq. (S17) is used:

$$uDF_{surf} = uDFtemp \times uDFwater \times uDFpH \qquad (S17)$$

Where uDF_{surf} is the decomposition modifier of C pools on the surface layer.

The decomposition modifier in the mineral soil layer is calculated following equation S18:

$$uDF_{soil} = uDF_{surf} \times uDFan \qquad (S18)$$

Where uDF_{soil} is the decomposition modifier of any C pools situated in the mineral soil layer, uDF_{surf} is from eq. (S17) above, and $uDFan$ is the anaerobic modifier from equation S13.

There are a few exceptions to the rules in equation S17 and S18: $SOM1$ in the mineral soil layer experience an additional sand effect $uDFsand$ i.e.:

$$uDF_{SOM12} = uDF_{soil} \times uDFsand \qquad (S19)$$

Where uDF_{SOM12} is the decomposition modifier of SOM1 in the mineral soil layer, uDF_{soil} is from equation S18, and $uDFsand$ is from equation S16.

Additionally, all lignin-containing detrital pools (structural litter and wood in both surface and mineral soil) experience further decomposition suppression as lignin content increases (it is not an "environmental" decomposition modifier per se):

$$uDFlig = \mathrm{e}^{(-kPligst \times frLig)} \qquad (S20)$$

Where uDF_{lig} is the lignin suppressive effect on decomposition rate, $kPligst$ is a parameter relating the lignin mass fraction $frLig$ to the decomposition of lignin-containing materials.

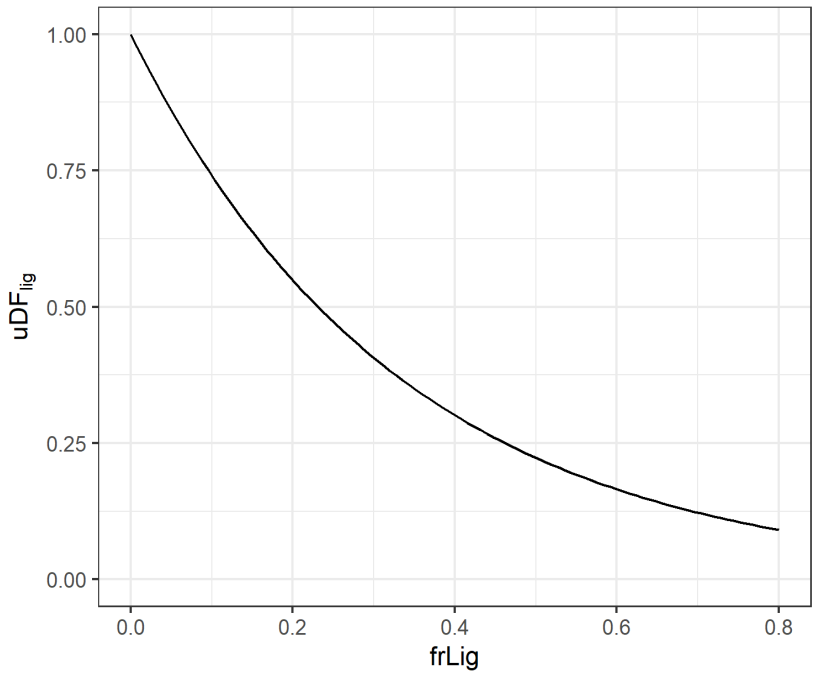

Figure S8: Decomposition rate modifier uDFlig as a function of the mass fraction of lignin (frLig).

Carbon flow in decomposition

Figure S5 earlier shows a schematic of how decomposition drives a transfer of C and N from one pool to another indicated by each arrow (CO_2 loss is also accompanying each transfer but is not shown in the figure).

Essentially, decomposition involves the loss of C from each state variable pool C_x i.e., $gTcflow_x$ in eq. (S2). $gTcflow_x$ is further sub-divided into 1) CO_2 produced from heterotrophic respiration $gCo2Los_x$ and 2) a transfer to the recipient pool C_y. The amount of heterotrophic CO_2 loss is calculated following equation S21.

$$gCo2Los_x = gTcflow_x \times kPC_xCO_2 \qquad (S21)$$

where $gCo2Los_x$ is the amount of heterotrophic CO_2 loss associated with the decomposition of C_x, $gTcflow_x$ is the total C flow during decomposition as calculated in equation S2, kPC_xCO_2 is a pool-specific parameter representing the fraction of C turned into CO_2 for each unit of C_x decomposed (Note that dynamic carbon use efficiency can be enabled, cf. eq. (S35), which replaces this parameter).

On the other hand, the amount of C transferred to recipient pool Cy is simply:

$$gCtransfer_{x,y} = gTcflow_x - gCo2Los_x \qquad (S22)$$

Where $gCtransfer_{x,y}$ is the amount of C transferred away from donor C pool x to recipient C pool y.

For SOM1 and SOM2 in the mineral soil, their decomposition transfers C into two recipient pools (SOM1 or SOM2, and SOM3). This is handled by an extra partitioning coefficient that represents the fraction of C flow to SOM3, controlled by clay content and anaerobic condition:

$$gCtransfer_{x,soc3} = gTcflow_x \times kFS_xS3 \times \left(1 + kAnimpt \times (1 - uDFan)\right) \qquad (S23)$$

Where $gCtransfer_{x,soc3}$ is the amount of C flowing into SOC3 pool, $kAnimpt$ is a linear parameter that relates $uDFan$ (eq. (S13) to $gCtransfer_{x,soc3}$ (more anaerobic or waterlogging = larger C transfer to SOC3 according to CENTURY), kFS_xS3 is a derived parameter dependent on clay content:

$$kFS_xS_3 = kPS_xS_31 + kPS_xS_32 \times kClay \qquad (S24)$$

Where kPS_xS_31 and kPS_xS_32 are the intercept and slope parameters relating clay fraction $kClay$ to kFS_xS_3. A higher kFS_xS_3 means more C is transferred to SOC3.

The flow to the second receiver pool is simply the remainder after subtracting C flow to SOC3 and CO_2.

In addition, the decomposition of lignin-containing materials (structural litter and wood) also flows into two pools (SOM1 and SOM2). However, no extra parameter is needed, it is assumed that the lignin portion ($frLig$) decomposes to SOM2 and the rest is decomposed into SOM1.

Bioturbation mixing of surface SOM2 to soil SOM2 (particulate organic matter)

Our model also considers the faunal bioturbation mixing of organic matter which transfers surface SOM2 to mineral soil SOM2. We used the equation developed in ForCent (Parton et al., 2010):

$$gTcflow_x = SOC2_{surf} \times kTmix \times uDF_{surf} \qquad (S25)$$

where $kTmix$ is the faunal mixing rate constant and uDF_{surf} is the decomposition modifier acting on surface layer (eq. (S17)). The transfer of SON2 is in direct accordance with the C:N ratio of surface SOC2 at the current timestep.

Nitrogen flow during decomposition

The amount of N transferred from the donor to the receiving pool are determined by two functions calculating the C:N ratios of organic matter entering the receiver pool C_y ($CNtransfer_y$), and $gCtransfer_{x,y}$ in eq. (S23). The functions for calculating $CNtransfer_y$ require parameters indicating the maximum and minimum C:N of the receiver pool ($maxCN_y$ and $minCN_y$), and the threshold N availability level above which $minCN_{receiver}$ applies. The actual N availability level at the current timestep is compared to this threshold N availability to calculate $CNtransfer_y$.

We used two functions (modified from CENTURY) to calculate $CNtransfer_y$, one for in-vivo microbial-derived organic matter (eq. (S26)) and another one for plant-derived organic matter decomposed ex-vivo (eq. (S27)) (Liang et al., 2017).

The first function ($called\ CEdrat1\ in\ the\ model\ code$) computes the C:N ratio for the decomposition of all OM pools going through in-vivo microbial processing (i.e., becoming or exiting microbial biomass pool SOC1). Only the decomposition of structural litter -> SOC2, Wood -> SOC2 (the ex-vivo plant matter decomposition pathways) are excluded. This C:N ratio for microbial-derived pools is calculated based on the amount of labile C and N present in soils:

$$CNtransfer_y = \begin{cases} minCN_y & \text{if } (\ gLabileCN_x \leq (minCN_y \div kCUEmax)) \\ \left(1 - \dfrac{minCN_y \div kCUEmax}{gLabileCN_x}\right) \times (maxCN_y - minCN_y) + minCN_y & \text{else} \end{cases} \qquad (S26)$$

Where $CNtransfer_y$ is a function of $gLabileCN_x$, the ratio of labile C and N pools during the current timestep (eq. (S32)), and $minCN_y$ - the minimum C:N of C_y divided by $kCUEmax$ – the theoretical maximum carbon use efficiency (Sinsabaugh et al., 2016), which together represent the labile C:N ratio at which minimum C:N is attained.

The second function ($called\ CEdrat2\ in\ the\ model\ code$) is used for the decomposition of structural litter -> SOC2 and Wood -> SOC2 (the plant-derived ex vivo pathway), based on the donor substrate original C:N ratio. This equation is taken from Century directly:

$$CNtransfer_y = \begin{cases} minCN_{reciever} & \text{if } \left(\frac{N_{donor}}{\left(C_{donor} \times \frac{1}{kCDF}\right)} > kN_{threshold} \right) \\ maxCN_{\mathrm{y}} + \frac{N_{donor}}{\left(C_{donor} \times \frac{1}{kCDF}\right)} \times \left(\frac{minCN_{\mathrm{y}} - maxCN_{\mathrm{y}}}{kN_{threshold}} \right) & \text{else} \end{cases} \quad (S27)$$

Where $CNtransfer_y$ is a function of the N:C ratio of donor OM pool at the current timestep N_{donor}/C_{donor}, $kCDF$ is the carbon mass fraction of organic matter, $kN_{threshold}$ is the parameter of threshold nitrogen content by weight above which $minCN_{\mathrm{y}}$ applies, $\frac{N_{\mathrm{donor}}}{\left(C_{\mathrm{donor}} \times \frac{1}{CDF}\right)}$) is basically the nitrogen content of the donor pool by weight.

From these calculated C:N ratios of organic matter flow into the receiver pool, the amount of N transferred into the receiver pool is simply:

$$gNtransfer_y = gCtransfer_{donor} \times \frac{1}{CNtransfer_y} \quad (S28)$$

Crucially, if $gNtransfer_y$ is larger than $gTnflow_x$ (the total amount of N flowing out of donor pool), immobilization occurs and the extra N required is taken from the state variable $MinerlN$ pool, vice versa for net mineralization to occur when $gNtransfer_y$ is smaller than $gTnflow_x$ and $MinerlN$ pool gains the excess N.

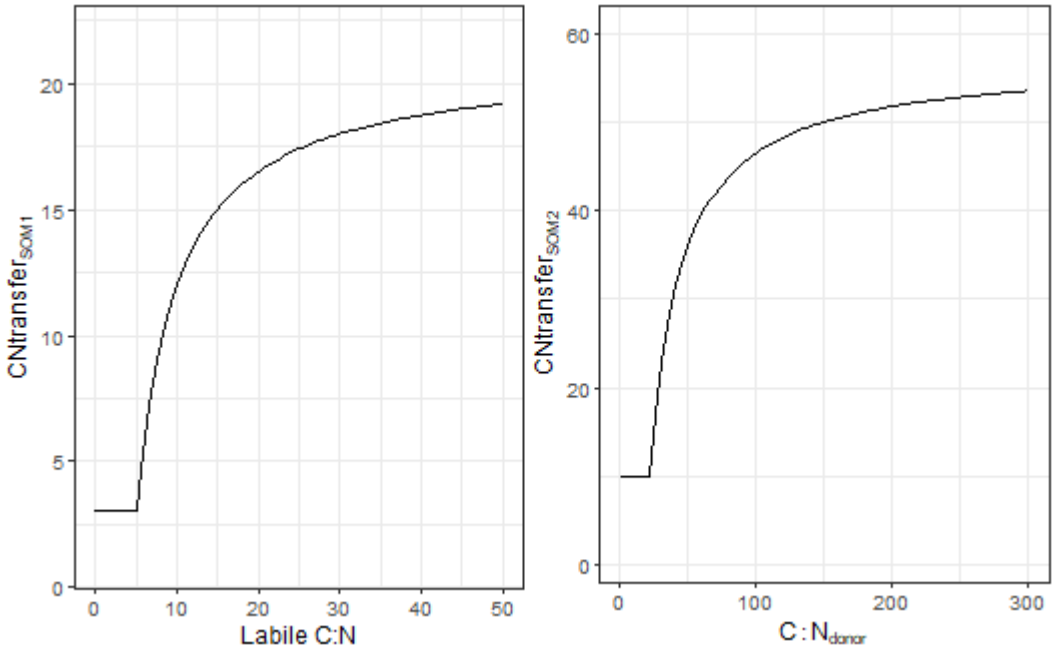

Figure S9: The relationship of CNtransfer$_{som1}$ and labile C:N calculated by CEdrat1 (eq. S26) and the relationship of CNtransfer$_{som2}$ and C:N$_{donor}$ calculated by CEdrat2 (eq. S27) .

New nitrogen-induced decomposer adaptive responses

N limitation constraint on the decomposition of lignin-containing materials

During the decomposition of high C:N substrates like deadwood and structural litter, there could be insufficient $MinerlN$ to satisfy immobilization requirement (when $C{:}\,N_{donor} >> maxCN_{receiver}$). This is a particular problem when we use deadwood litter produced from forest models with explicit mortality, resulting in high C:N deadwood being added to soil in big discrete pulses. Default CENTURY does not have a mechanism to handle this (when this happens, it results in unrealistically high C:N ratio of the receiver pools above $maxCN_{receiver}$). Hence, we added a N limitation constraint based on mass balance (eq. (S29)) to reduce C decomposition based on the total amount of N available to decomposer ($N_{donor} + MinerlN$) (cf. Manzoni & Porporato, 2009, section 3.4). This simultaneously represents a stimulatory effect of N addition on the decomposition of N-limited substrates, which is supported by literature evidence (Allison et al., 2009, Jing et al., 2021).

$$\text{if}(gNdiff < 0) \qquad gTcflow\_red_x = \frac{gNdiff \times CN_{donor}}{(CN_{donor}/CNtransfer_{receiver}) - 1} \qquad (S29)$$

where $gTcflow\_red_x$ is the amount of C to be subtracted from $gTcflow_x$ (eq. S2) based on the shortage of microbially-available N ($gNdiff$, eq. S30), i.e., more N alleviates the shortage and lowers $gTcflow\_red_x$. CN_{donor} is the C:N ratio of the decomposing pool, $CNtransfer_{receiver}$ is the calculated C:N ratio of new materials entering the receiver pool (eq. S26 & S27). The equation is derived algebraically and respects exact mass balance. $gNdiff$ is calculated as:

$$gNdiff = (MinerlN_i + gTcflow_x/CN_{donor}) - (gTcflow_x/CNtransfer_{receiver}) \qquad (S30)$$

where $MinerlN_i$ is the Minerl N pool in the current layer *i* of the decomposing pool.

Nitrogen decomposition retardation factor under excess nitrogen

Excess N supply (relative to C) can retard the decomposition of 1) lignin-containing or lignin-derived organic matter (e.g., StrucC, Wood1C, SOC2 in CENTURY), and 2) protein-rich low C:N organic matter (e.g., SOC3 in CENTURY), by regulating the production of oxidase and peptidase enzymes. To capture this, we implemented a decomposition modifier (eq. (S31)) to reduce decomposition rate linearly under excess N until a maximum reduction when labile C:N reaches zero (n.b. being linear with respect to labile C:N – TER means being non-linear with respect to N addition rate). This modifier is multiplied to the decomposition rate same as the other environmental decomposition modifiers.

$$gNDRF_x = \begin{cases} 1 & \text{if } ((gLabileCN_x - gTER_i) > 0) \\ 1 + \left((1 - kNDRFmin_s) \times \frac{(gLabileCN_x - gTER_i)}{gTER_i} \right) & \text{if } ((gLabileCN_x) < gTER_i \text{ and } gLabileCN_x > 0) \\ kNDRFmin_s & \text{if } (gLabileCN_x = 0) \end{cases} \quad (S31)$$

where $gNDRF_x$ is the excess-N decomposition retardation effect for each susceptible C_x (Fig. S5). $kNDRFmin_s$ is the maximum decomposition reduction (lowest value) for each OM type s (either lignin-containing materials i.e., StrucC, Wood1C and SOC2, or proteinaceous material i.e., SOC3). Two dynamic variables are calculated monthly to control the extent of decomposition reduction, 1. labile C:N supply ($gLabileCN_x$), and 2. microbial C:N demand ($gTER_i$). The lower $gLabileCN_x$ is relative to $gTER_i$, the stronger the effect is.

$$gLabileCN_x = \frac{(MetabC_i + gTcflow_x)}{(MetabN_i + MinerlN_i + gTnflow_x)} \quad (S32)$$

where the numerator is the sum of all labile C consisting of $MetabC_i$ – the most labile C pool in layer i and $gTcflow_x$ – the potential amount of decomposition C flow from C_x before any N-induced decomposition retardation applies. The denominator is the same but with N, plus an additional mineral N pool. $gLabileCN_x$ is calculated for every instance of C pool decomposition and hence implicitly accounts for C and N resource heterogeneity in the soil micro-environment.

$gTER_i$ is calculated by the formula below:

$$gTER_i = \frac{(SOC1_i/SON1_i)}{kCUEmax} \quad (S33)$$

where $SOC1_i/SON1_i$ represents the C:N ratio of microbial biomass in soil layer i , and $kCUEmax$ is the theoretical maximum CUE achievable under ideal conditions (Sinsabaugh et al., 2016). We assumed that maximum N use efficiency is equal to 1 and can thus be omitted from the equation (Cui et al., 2023). The model only calculates $gTER_i$ per layer because microbial biomass C:N (i.e., TER) is inherently less variable than labile C:N.

Nitrogen-induced effect on microbial turnover rate and CUE

Many studies reported microbial biomass reduction under increasingly excessive N, which was correlated with reduced decomposition rate. There are two possible explanations of reduced microbial biomass: 1) Increase in microbial turnover rate due to a shift to copiotrophic community under N-rich conditions (Fierer et al., 2011); 2) Reduced CUE under intensifying stoichiometric imbalance i.e., either excess N or excess C relative to $gTER_i$ (Manzoni et al., 2010, Sinsabaugh et al.,2016).

Hence, we made the turnover rate parameter $kDec3_i$ of the microbial pool SOC1 into a dynamic variable dependent on $SOC1_i/SON1_i$, where a low C:N ratio is associated with a microbial community dominated by copiotrophs which has fast turnover and vice versa for oligotrophs. Based on literature estimates (Rousk & Bååth, 2011), we assume the turnover rate of copiotrophs at the lowest microbial biomass C:N ratio to be four times that of the

slowest-turnover oligotroph. From this, we can derive the minimum $kDec3min_i$ and maximum $kDec3max_i$ microbial turnover rate (which have four-fold differences) algebraically using the default turnover rate parameter $kDec3$ as the mid-point. This range of turnover rates from min to max is made to linearly varies between the maximum ($kVarat1_1$) and minimum C:N of microbial biomass ($kVarat1_2$):

$$gDec3_i = kDec3min_i + \left(kVarat1_1 - (SOC1_i/SON1_i)\right) \times \frac{(kDec3max_i - kDec3min_i)}{(kVarat1_1 - kVarat1_2)} \qquad (S34)$$

where $gDec3_i$ is the dynamic monthly turnover rate of SOC1 (microbes) of layer i, $kDec3min_i$ and $kDec3max_i$ are the minimum and maximum turnover rate parameters corresponding to fully oligotrophic and copiotrophic microbial communities, respectively (Rousk & Bååth, 2011), calculated from the ratio of the turnover rate of copiotrophs versus oligotrophs (Appendix 2). $kVarat1_1$ and $kVarat1_2$ are the maximum and minimum C:N of the microbial pool, respectively.

Secondly, instead of considering a constant CUE across time as in default CENTURY (i.e., $1 - kPC_xCO_2$ is a parameter, see eq. (S21)), we introduced dynamic CUE responsive to the stoichiometric imbalance between labile C:N and TER, approximating the stoichiometric theory by Sinsabaugh et al. (2016). Essentially, CUE decreases in response to an increasing deviation of labile C:N from TER as in $gNDRF_x$ (eq. (S31)) until a minimum CUE is reached:

$$gCUE_x = \begin{cases} kCUEmax & \text{if } (gLabileCN_x - gTER_i = 0) \\ kCUEmax - \frac{(kCUEmax - kCUEmin)}{gTER_i} \times (|gLabileCN_x - gTER_i|) & \text{if } (0 < |gLabileCN_x - gTER_i| < gTER_i) \\ kCUEmin & \text{if } (|gLabileCN_x - gTER_i| > gTER_i) \end{cases} \qquad (S35)$$

where $gCUE_x$ is the microbial carbon use efficiency for the current decomposition (x can be MetabC, StrucC, WoodC, SOC2, SOC3 that decompose to form SOC1), $kCUEmax$ and $kCUEmin$ are parameters constraining the theoretical maximum and minimum CUE respectively. Theoretically, changing CUE is also viewed as one of the homeostatic adaptations for microbes to handle nutrient limitation via C overflow (Manzoni & Porporato, 2009).

Microbial biomass control on decomposition (priming)

Both the dynamic CUE and dynamic turnover rate feedback into the production of microbial biomass and necromass. The altered microbial biomass may further exert an impact on decomposition. We formulated an equation representing the microbial biomass effect on decomposition using relative microbial biomass $gRelMBC_i$ i.e. the ratio of realized microbial biomass (SOC1) to total labile C resources potentially convertible to microbial biomass as an explanatory variable:

$$gRelMBC_i = \frac{SOC1_{i,m}}{\sum_{x,i} C_{x,,m-1} \times kDec\_rel_{x,i} \times gCUE_{x,m-1}} \qquad (S36)$$

where the denominator is the sum of all C pools (except SOC1) in the last month (*m-1*) in soil layer i multiplied with their respective relative turnover rates $kDec\_rel_{x,i}$ and most recent carbon use efficiency $gCUE_{x,m-1}$. $kDec\_rel_{x,i}$ is defined as the ratio of the decomposition rate parameter of each C pool x relative to the decomposition rate parameter of metabolic litter (the most labile C) in the same layer i.e., it extracts the labile portion of each C substrate.

Finally, the microbial biomass effect on decomposition is calculated as:

$$gMB\_eff_i = \left(kPrimemax - e^{\left(-\ln\left(\frac{kPrimemax}{kPrimemax-1}\right)\right)\times gRelMBC_i + \ln(kPrimemax)} \right) \qquad (S37)$$

where gMB_eff_i is a logistic function representing the microbial biomass decomposition effect at layer i, multiplied to decomposition rate just as the other decomposition modifiers. $kPrimemax$ is a parameter representing the maximum monthly priming effect. This formulation has the property of passing through 1 at $gRelMBC_i = 1$ and could model both positive and negative priming when $gRelMBC_i$ is bigger or smaller than 1 respectively.

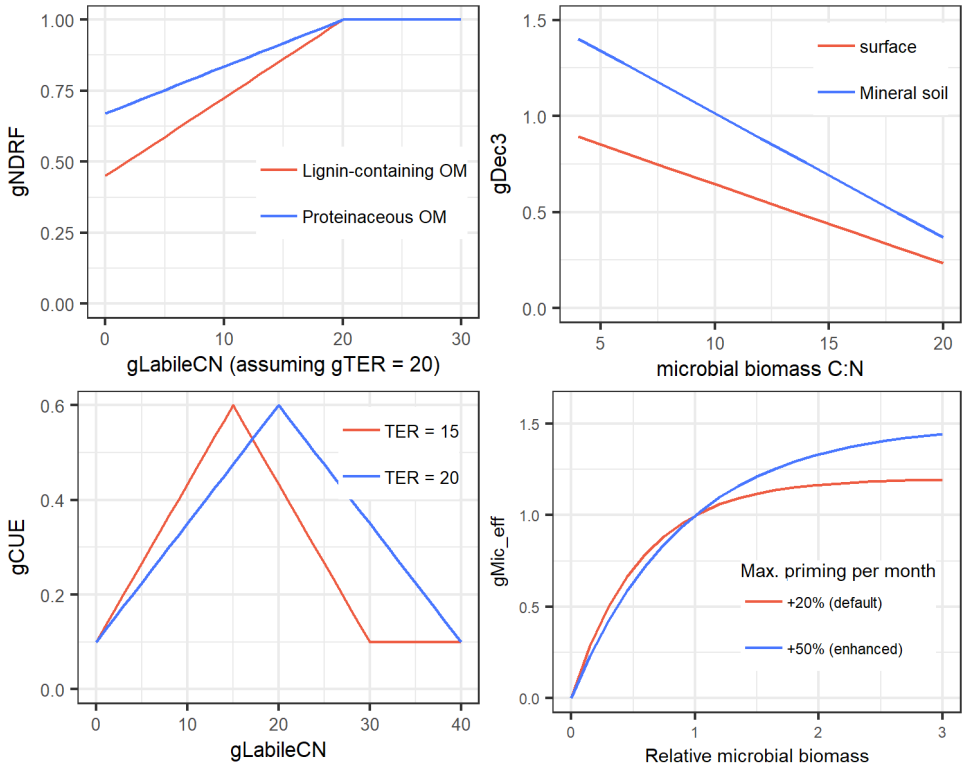

Figure S10: New nitrogen-driven microbial adaptive responses: gNDRF, gDec3, gCUE, gMB_eff as functions of gLabileCN, gTER, MBC:N and relative microbial biomass.

Boundary mineral nitrogen flux

Mineral N is the key control of the above new N effects (eq. S31-S37) as well as being the key connection between the soil and plant models. Boundary N fluxes encompass N fluxes in and out of the $MinerlN$ state variable pool.

There are two ways where $MinerlN$ is gained aside from the mineralization of organic matter:

1. N-deposition, where it is separated into historical and contemporary N-deposition. The latter is an external input based on measured data and does not require endogenous calculation. For historical N deposition ($gNdep$), we adopted the equation in CENTURY based on annual precipitation:

$$gNdep_m = (kEpnfa1 + kEpnfa2 \times uArain) \times uP_m/uP_{an}; \qquad (S38)$$

where $kEpnfa1$ and $kEpnfa2$ are intercept and slope parameters that relate N-deposition to precipitation. $uArain$ is the long-term average annual precipitation in cm (capped to a maximum of 80cm), uP_m is the precipitation in the current month and uP_{an} is the precipitation in the current year (Bugmann, 1994). uP_m/uP_{an} is essentially a fraction to allocate the estimated annual N deposition to monthly portions.

2. N-fixation, calculated based on the central estimate empirical equation in Cleveland et al. (1999):

$$gNfix_m = (0.234 \times AET_{an} - 0.172)/10 \times AET_m/AET_{an}; \qquad (S39)$$

where AET_{an} and AET_m are actual evapotranspiration of the current year and month, respectively, AET_m/AET_{an} is a fraction used to allocate annual N fixation to every month.

Nitrogen deposition ($gNdep_m$) is currently deposited at the $MinerlN$ pool of the surface layer immediately, in accordance with tracer experiments showing that most deposited N is retained in the litter and organic layer over short-term submonthly scale (Templer et al., 2012). Similarly, fixed nitrogen is also added to the $MinerlN$ pool of the surface layer (Lladó et al., 2017). The subsequent transfer of N to the mineral soil layer below over longer timescales is handled by leaching.

Next, $MinerlN$ is lost via two pathways at the end of each month:

1. A layer-specific leaching loss of nitrogen based on the amount of water going in and out of a layer, as well as soil clay content.

2. A transpiration-driven plant uptake removing N from the whole soil profile.

Leaching does not occur if the amount of water going into a layer is less than its remaining water retention capacity. On the contrary, when water influx is in excess of the retention capacity, leaching occurs according to the following layer-specific equations. For the surface layer:

$$gLeachN_{m,surf} = MinerlN \times \frac{uLeachW_{m,surf}}{uPa_m} \qquad (S40)$$

where $gLeachN_{m,surf}$ is the mineral N (gNm^{-2}) transferred from the surface layer to the soil layer below, $uLeachW_{m,surf}$ (cm) is the amount of water exceeding the water-holding capacity and leached downward from the surface into mineral soil, uPa_m (cm) is the total water influx into the soil including throughfall flux and snow melt water in the current month *m* (Huber et al., 2020).

For the mineral topsoil layer,

$$gLeachN_{m,soil} = MinerlN \times \left(\frac{uLeachW_{m,soil}}{uLeachW_{m,surf} + \left(SM_{m-1} \times \frac{gBS_{soil}}{kBS}\right)} \times (1 - kClay)\right) \qquad (S41)$$

where $gLeachN_{m,soil}$ is the mineral N transferred from the topsoil layer (20cm) to the deep soil layer below (n.b. elements in the deep layer are assumed lost from the system in this study, as we only simulated the surface organic horizon and topsoil layers), $uLeachW_{m,soil}$ (cm) is the amount of water leached downward from the topsoil layer to the deep soil layer (after subtracting evapotranspiration flux uE_m), SM_{m-1} is the remaining soil water (cm) in the topsoil layer from the previous month, gBS_{soil} and kBS are the soil water-holding capacity of topsoil layer and the whole profile, respectively.

The $uLeachW$ variables are calculated by mass balance (i.e., total water influx into a layer plus soil water remaining from the previous month, minus layer-specific water-holding capacities). We denote the water-holding capacity (field capacity - wilting point) of the surface organic layer, 20cm topsoil layer, and the whole soil profile as gBS_{surf}, gBS_{soil} and kBS (a model input parameter) respectively. gBS are updated annually according to the following eq. (S42) and (S43):

$$gBS_{surf} = kBS\_spec_{LFH} \times \frac{TotC_{surf,m}}{kCDF} \qquad (S42)$$

Where kBS_spec_{LFH} is the mass-specific water holding capacity of surface layer organic matter in cm g^{-1} dry mass of organic matter (Zagyvai-Kiss et al., 2019), $TotC_{surf,m}$ is the sum of all the organic C pools (except deadwood) in the surface layer (MetabC, StrucC, SOC1, SOC2) and $kCDF$ is the carbon mass fraction of soil organic matter. For mineral topsoil:

$$gBS_{soil} = (gAfiel - gAwilt) \times kAdep_{soil} \qquad (S43)$$

where $gAfiel$ and $gAwilt$ are estimated field capacity at -0.1 bar and wilting point at -15 bar (in volumetric fraction) respectively, using Rawls's pedotransfer equations bundled with CENTURY (Rawls et al., 1982). $kAdep$ is the depth of topsoil layer in cm, which is fixed at 20cm.

With these layer-specific water-holding capacities, $uLeachW_{m,surf}$ and $uLeachW_{m,soil}$ are then calculated:

$$uLeachW_{m,surf} = uPa_m - gBS_{surf} \quad (S44)$$

$$uLeachW_{m,soil} = (uLeachW_{m,surf} + (SM_{m-1} - uE_m) \times \frac{gBS_{soil}}{kBS}) - gBS_{soil} \quad (S45)$$

Where uPa_m (cm) is the total water influx into soil including throughfall flux and snow melt water (Huber et al., 2020), SM_{m-1} is the remaining soil water (cm) in the topsoil layer from the previous month, uE_m (cm) is the estimated evapotranspiration flux from soil through vegetations, $\frac{gBS_{soil}}{kBS}$ is a fraction allocating soil water to the topsoil relative to the whole profile. Note that we calculate $uLeachW_{m,surf}$ before and $uLeachW_{m,soil}$ after evapotranspiration water loss, due to the short timescale of leaching from surface litter layer.

Secondly, transpiration N loss from soil (≈ plant uptake) occurs uniformly across $MinerlN$ pools of all layers:

$$gNloss_m = \frac{uE_m}{(uPa_m + SM_{m-1})} \quad (S46)$$

where $gNloss_m$ is the fraction of mineral N loss of any layer due to transpiration uptake, uE_m (cm) is the estimated evapotranspiration flux from soil through vegetations, uPa_m (cm) is the total water influx into soil including throughfall flux and snow melt water, SM_{m-1} is the remaining soil water (cm) in the topsoil layer from the previous month.

Note that mineral N loss by denitrification is implicit, because the N gases released from the soil water stream only lowers the concentration of N in solution.

List of model parameters

Parameter name	Description	Value	References
Initial value of state variables (g/m^2). Two values indicate different soil layers.			
MetabC$_i$†	C stock of metabolic litter	88, 280 (surface, mineral soil)	ForCent default*
MetabN$_i$	N stock of metabolic litter	2.65, 8.5	ForCent default*
StrucC$_i$	C stock of structural litter	312, 420	ForCent default*
StrucN$_i$	N stock of structural litter	1.56, 2.1	ForCent default*
Wood1C$_i$	C stock of deadwood	0, 0	ForCent default*
Wood1N$_i$	N stock of deadood	0, 0	ForCent default*
SOC1$_i$	C stock of SOM1 (fast-cycling organic matter)	105, 120	ForCent default*
SON1$_i$	N stock of SOM1 (fast-	7.5, 11.4	ForCent default*

	cycling organic matter)		
$SOC2_i$	C stock of SOM2 (intermediate-cycling organic matter)	1400, 1800	ForCent default*
$SON2_i$	N stock of SOM2 (intermediate-cycling organic matter)	53, 69	ForCent default*
$SOC3_i$	C stock of SOM3 (slow-cycling organic matter)	0, 1200	ForCent default*
$SON3_i$	N stock of SOM3 (slow-cycling organic matter)	0, 92	ForCent default*
$MinerlN_i$		1.56, 0.18	ForCent default*
SOM decomposition model parameters. Two values indicate different soil layers.			
$kDec1_i$	Maximum decomposition rate of structural litter (y^{-1}) ‡	2.5, 4.9 (surface, mineral soil)	ForCent default*
$kDec2_i$	Maximum decomposition rate of metabolic litter (y^{-1})	10, 18.5	ForCent default*
$kDec3_i$	Maximum decomposition rate of SOM1 (y^{-1})	7, 11	ForCent default*
$kDec4_i$	Maximum decomposition rate of SOM2 (y^{-1})	0.16, 0.46	ForCent default*
kDec5	Maximum decomposition rate of SOM3 (y^{-1})	0.0025 or 0.0068	ForCent and CENTURY default, evaluated in base model test
$kDecw_i$	Maximum decomposition rate of coarse deadwood (y^{-1})	0.5, 0.6	ForCent default*
kTmix	Maximum mixing rate of surface SOC2 to soil SOC2 ($month^{-1}$)	0.22	ForCent default*
kTeff1	Shape parameter 1 of the arctangent function of temperature effect on decomposition	15.4	ForCent default*
kTeff2	Shape parameter 2 of the arctangent function of temperature effect on decomposition	11.75	ForCent default*
kTeff3	Shape parameter 3 of the arctangent function of temperature effect on decomposition	29.7	ForCent default*
kTeff4	Shape parameter 4 of the arctangent function of	0.031	ForCent default*

	temperature effect on decomposition		
kWeff1	Shape parameter 1 of the logistic function of soil moisture effect on decomposition	10	ForCent default*
kWeff2	Shape parameter 2 of the logistic function of soil moisture effect on decomposition	-6	ForCent default*
kPheff1	Shape parameter 1 of the arctangent function of pH effect on decomposition	4 (mixed), 3 (fungal), 4.8 (bacterial) §	CENTURY v4.6 default*
kPheff2	Shape parameter 2 of the arctangent function of pH effect on decomposition	0.5	CENTURY v4.6 default*
kPheff3	Shape parameter 3 of the arctangent function of pH effect on decomposition	1.1	CENTURY v4.6 default*
kPheff4	Shape parameter 4 of the arctangent function of pH effect on decomposition	0.7	CENTURY v4.6 default*
kANeff1	The ratio of water input to potential evapotranspiration (RPRPET), below which there is no anaerobic effect on decomposition	1.5	ForCent default*
kANeff2	The ratio of water input to potential evapotranspiration (RPRPET), at or above which there is maximum anaerobic effect on decomposition	3	ForCent default*
kANeff3	Maximum decomposition suppressive effect at or above kAneref2	0.3	ForCent default*
kAnimpt	Slope parameter used to control the impact of soil anaerobic conditions on decomposition C flow to SOM3	5	ForCent default*

kDrain	Parameter representing drainage efficiency that controls the anaerobic effect on decomposition	Site-specific sand fraction	User-defined parameter
kSeff1	Intercept term for the sand-induced decomposition rate modifier of soil SOC1	0.25	ForCent default*
kSeff2	Slope term for the sand-induced decomposition rate modifier of soil SOC1	0.75	ForCent default*
kPligst	The exponent multipler that determines the effect of lignin content on structural and wood litter decomposition	3	ForCent default*
$kP1CO2A_i$	Intercept parameter controlling the fraction of C lost from SOC1 to CO_2 during decomposition, at sand content = 0	0.6, 0.17	ForCent default*
$kP1CO2B_i$	Slope parameter controlling the fraction of C flow from SOC1 to CO_2 based on sand fraction	0, 0.68	ForCent default*
$kP2CO2_i$	The fraction of C flow becoming CO_2 during SOC2 decomposition	0.55, 0.55	ForCent default*
kP3CO2	The fraction of C flow becoming CO_2 during SOC3 decomposition	0.55	ForCent default*
$kPMCO2_i$	The fraction of C flow becoming CO_2 during metabolic litter decomposition	0.55,0.55	ForCent default*
$kPS1CO2_i$	The fraction of C flow becoming CO_2 during structural litter decomposition	0.45, 0.55	ForCent default*
$kPS1S3_1$	Intercept parameter controlling the fraction of C flow from SOC1 to SOC3 at clay content = 0	0.003	ForCent default*
$kPS1S3_2$	Slope parameter	0.032	ForCent default*

	controlling the fraction of C flow from SOC1 to SOC3 based on clay fraction		
$kPS2S3_1$	Intercept parameter controlling the fraction of C flow from SOC1 to SOC3 at clay content = 0	0.003	ForCent default*
$kPS2S3_2$	Slope parameter controlling the fraction of C flow from SOC1 to SOC3 based on clay fraction	0.009	ForCent default*
$kPcemic1_1$	Maximum C:N of surface microbial biomass (SOC1)	21	Gao et al., 2022
$kPcemic1_2$	Minimum C:N of surface microbial biomass (SOC1)	3	Gao et al., 2022
$kPcemic1_3$	Threshold concentration of nitrogen in the donor C pool above which minimum C:N ($kPcemic1_2$) applies	0.02	ForCent default*
$kPcemic2_1$	Maximum C:N of surface SOC2	57	LUCAS POC and PON data (Lugato et al., 2021)
$kPcemic2_2$	Minimum C:N of surface SOC2	12	LUCAS POC and PON data (Lugato et al., 2021)
$kVarat1_1$	Maximum C:N of soil microbial biomass (SOC1)	21	Gao et al., 2022
$kVarat1_2$	Minimum C:N of soil microbial biomass (SOC1)	3	Gao et al., 2022
$kVarat2_1$	Maximum C:N of soil POM (SOC2)	57	LUCAS POC and N data (Lugato et al., 2021)
$kVarat2_2$	Minimum C:N of soil POM (SOC2)	12	LUCAS POC and N data (Lugato et al., 2021)
$kVarat3_1$	Maximum C:N of soil MAOM (SOC3)	27	LUCAS MAOC and N data (Lugato et al., 2021)
$kVarat3_2$	Minimum C:N of soil MAOM (SOC3)	6	LUCAS MAOC and N data (Lugato et al., 2021)
New N decomposition effect parameters			
$kNDRFmin_s$¶	Maximum decomposition retardation effect at labile C:N = 0, for	Lignin-rich material: 0.55, Protein-rich material: 0.67	H. Chen et al., 2018; J. Chen et al., 2018; 10th percentile values.

	either: 1. lignin-containing OM, or 2. Protein-rich low C:N OM		
kDec3_rat	The ratio of the turnover rates of copiotrophs to oligotrophs	4	Rousk & Bååth, 2011
kCUEmin	Minimum CUE	0.05	Sinsabaugh et al., 2015
kCUEmax	Maximum CUE	0.6	Sinsabaugh et al., 2015, 2016
kPrimemax	Maximum monthly priming effect multiplier	1.25 (25% increase in monthly decomposition rate at maximum priming)	Luo et al., 2016
Boundary nitrogen flux parameters			
kEpnfa1	Intercept term for background N deposition when annual precipitation is zero	0.05	ForCent default*
kEpnfa2	Slope term relating historical N deposition to annual precipitation	0.007	ForCent default*
kBS_spec_LFH	Specific water-holding capacity (cm) of the surface horizon per unit weight of litter mass (g)	0.00021	Zagyvai-Kiss et al., 2019
Litter production parameters			
kSpl1	Intercept term for fraction partitioned to metabolic litter when lignin:N is zero	0.85	ForCent default*
kSpl2	Slope term relating the fraction partitioned to metabolic litter to lignin:N	0.013	ForCent default*
kCNs	Fixed C:N ratio of structural litter	200	ForCent default*
kConv	Empirical conversion factor converting basal area to twig litter production	0.0025	ForClim v4.0.1 default (Huber et al., 2021)
$kFRT_s$¶	Foliage retention time (y) for either deciduous or evergreen species	Decid: 1, evergreen:5	ForClim v4.0.1 default (Huber et al., 2021)
kRSR	Empirical ratio for the amount of fine root litter (down to 20cm depth) to foliage litter	0.9	Brunner et al., 2013; Keller et al., 2021; Leppälammi-Kujansuu, Aro, et al., 2014;

			Leppälammi-Kujansuu, Salemaa, et al., 2014; Leuschner et al., 2004
kRER	Empirical ratio for the amount of root exudates to fine root litter	0.1	Phillips et al., 2011; Tückmantel et al., 2017; Wang et al., 2021
kRBwAw	Ratio of coarse belowground deadwood to aboveground deadwood	0.2	He et al., 2018; Kurz et al., 1996
kCDF	Carbon fraction of plant biomass	0.48	ICP-II forest measurement (Thimonier et al., 2001)
$kCNf_{kLQ}^{\#}$	The C:N ratio of foliage litter (differentiated by three litter quality classes kLQ)	40,55,70	Kang et al., 2010; Yuan & Chen, 2009
kCNr	The C:N ratio of fine root litter	48	Jackson et al., 1997; Liang et al., 2018
kCNt	The C:N ratio of twig litter	55	ICP-II forest measurement (Thimonier et al., 2001)
kCNex	The C:N ratio of root exudates	13.5	Cai et al., 2022; Z. Zhang et al., 2016
$kCNw1_{kLQ}$	The C:N ratio of coarse woody litter (differentiated by three litter quality classes kLQ)	221, 393, 515	Weedon et al., 2009
$kLigf1_{kLQ}$	The lignin fraction of foliage litter (differentiated by three litter quality classes kLQ)	0.15, 0.25, 0.3	Scott & Binkley, 1997; X. Zhang & Wang, 2015
kLigr	The lignin fraction of fine root litter	0.25	Iversen et al., 2017
kLigt	The lignin fraction of twig litter	0.25	Pei et al., 2019; Tu et al., 2014
$kLigw1_{kLQ}$	The lignin fraction of coarse woody litter (differentiated by three litter quality classes kLQ)	0.17, 0.215, 0.275	Weedon et al., 2009

*Based on ForCent parameters (Parton et al., 2010)

† Parameter with the *i* subscript contain values corresponding to two different soil layers. The first value corresponds to the surface organic horizon, whereas the second value corresponds to the first 20cm of the mineral soil.

‡ ForCent by default reports their "decomposition rate parameters" in y^{-1}, but in the model, the rate parameters are divided by 12 to obtain a $month^{-1}$ value for calculating decomposition monthly.

§ According to CENTURY v4.6, SOM1 in the mineral soil and all metabolic litter are bacterially decomposed, and SOM3 is fungally decomposed, with respect to the pH retardation effect. All the other C pools are decomposed by a mix of bacteria and fungi with kPheff1 = 4 (also for bioturbation pH effect).

¶ Parameter with the *s* subscript contain values corresponding to different types (species) of organic matter. In the case of $kFRT_s$, the subscript represents the foliage retention time of either deciduous or evergreen species.

Parameter with the *kLQ* subscript contain values corresponding to different classes of litter quality.

References

Bugmann, H. (1994). On the ecology of mountainous forests in a changing climate: a simulation study (Doctoral dissertation, ETH Zurich).

Berardi, D. M., Hartman, M. D., Brzostek, E. R., Bernacchi, C. J., DeLucia, E. H., von Haden, A. C., ... & Parton, W. J. (2024). Microbial-explicit processes and refined perennial plant traits improve modeled ecosystem carbon dynamics. *Geoderma*, *443*, 116851.

Brunner, I., Bakker, M. R., Björk, R. G., Hirano, Y., Lukac, M., Aranda, X., Børja, I., Eldhuset, T. D., Helmisaari, H. S., Jourdan, C., Konôpka, B., López, B. C., Miguel Pérez, C., Persson, H., & Ostonen, I. (2013). Fine-root turnover rates of European forests revisited: An analysis of data from sequential coring and ingrowth cores. *Plant and Soil*, *362*(1), 357–372. https://doi.org/10.1007/s11104-012-1313-5

Cai, G., Shahbaz, M., Ge, T., Hu, Y., Li, B., Yuan, H., Wang, Y., Liu, Y., Liu, Q., Shibistova, O., Sauheitl, L., Wu, J., Guggenberger, G., & Zhu, Z. (2022). Root exudates with low C/N ratios accelerate CO emissions from paddy soil. *Land Degradation & Development*, *33*(8), 1193–1203. https://doi.org/10.1002/ldr.4198

Chen, H., Li, D., Zhao, J., Xiao, K., & Wang, K. (2018). Effects of nitrogen addition on activities of soil nitrogen acquisition enzymes：A meta-analysis. *Agriculture, Ecosystems & Environment*, *252*, 126–131. https://doi.org/10.1016/j.agee.2017.09.032

Chen, J., Luo, Y., van Groenigen, K. J., Hungate, B. A., Cao, J., Zhou, X., & Wang, R. (2018). A keystone microbial enzyme for nitrogen control of soil carbon storage. *Science Advances*, *4*(8), eaaq1689. https://doi.org/10.1126/sciadv.aaq1689

Cleveland, C. C., Townsend, A. R., Schimel, D. S., Fisher, H., Howarth, R. W., Hedin, L. O., … & Wasson, M. F. (1999). Global patterns of terrestrial biological nitrogen (N2) fixation in natural ecosystems. *Global biogeochemical cycles*, 13(2), 623-645.

Cui, Y., Moorhead, D. L., Peng, S., & Sinsabaugh, R. L. (2023). New insights into the patterns of ecoenzymatic stoichiometry in soil and sediment. *Soil Biology and Biochemistry*, *177*, 108910. https://doi.org/10.1016/j.soilbio.2022.108910

Del Grosso, S. J., W. J. Parton, A. R. Mosier, E. A. Holland, E. Pendall, D. S. Schimel, and D. S. Ojima. 2005. Modeling soil CO2 emissions from ecosystems. *Biogeochemistry* 73:71-91.

Gao, D., Bai, E., Wang, S., Zong, S., Liu, Z., Fan, X., Zhao, C., & Hagedorn, F. (2022). Three-dimensional mapping of carbon, nitrogen, and phosphorus in soil microbial biomass and their stoichiometry at the global scale. *Global Change Biology*, *28*(22), 6728–6740. https://doi.org/10.1111/gcb.16374

He, H., Zhang, C., Zhao, X., Fousseni, F., Wang, J., Dai, H., Yang, S., & Zuo, Q. (2018). Allometric biomass equations for 12 tree species in coniferous and broadleaved mixed forests, Northeastern China. *PLOS ONE*, *13*(1), e0186226. https://doi.org/10.1371/journal.pone.0186226

He, H., Zhang, C., Zhao, X., Fousseni, F., Wang, J., Dai, H., … & Zuo, Q. (2018). Allometric biomass equations for 12 tree species in coniferous and broadleaved mixed forests, Northeastern China. *PloS one*, 13(1), e0186226.

Huber, N., Bugmann, H., & Lafond, V. (2020). Capturing ecological processes in dynamic forest models: why there is no silver bullet to cope with complexity. *Ecosphere*, *11*(5), e03109.

Huber, N., Bugmann, H., Cailleret, M., Bircher, N., & Lafond, V. (2021). Stand-scale climate change impacts on forests over large areas: Transient responses and projection uncertainties. *Ecological Applications*, *31*(4), e02313. https://doi.org/10.1002/eap.2313

Iversen, C. M., McCormack, M. L., Powell, A. S., Blackwood, C. B., Freschet, G. T., Kattge, J., Roumet, C., Stover, D. B., Soudzilovskaia, N. A., Valverde-Barrantes, O. J., van Bodegom, P. M., & Violle, C. (2017). A global Fine-Root Ecology Database to address below-ground challenges in plant ecology. *New Phytologist*, *215*(1), 15–26. https://doi.org/10.1111/nph.14486

Jackson, R. B., Mooney, H. A., & Schulze, E.-D. (1997). A global budget for fine root biomass, surface area, and nutrient contents. *Proceedings of the National Academy of Sciences*, *94*(14), 7362–7366. https://doi.org/10.1073/pnas.94.14.7362

Kang, H., Xin, Z., Berg, B., Burgess, P. J., Liu, Q., Liu, Z., Li, Z., & Liu, C. (2010). Global pattern of leaf litter nitrogen and phosphorus in woody plants. *Annals of Forest Science*, *67*(8), 811.

Keller, A. B., Brzostek, E. R., Craig, M. E., Fisher, J. B., & Phillips, R. P. (2021). Root-derived inputs are major contributors to soil carbon in temperate forests, but vary by mycorrhizal type. *Ecology Letters*, *24*(4), 626–635. https://doi.org/10.1111/ele.13651

Kurz, W. A., Beukema, S. J., & Apps, M. J. (1996). Estimation of root biomass and dynamics for the carbon budget model of the Canadian forest sector. *Canadian Journal of forest research*, 26(11), 1973-1979.

Leppälammi-Kujansuu, J., Aro, L., Salemaa, M., Hansson, K., Kleja, D. B., & Helmisaari, H.-S. (2014). Fine root longevity and carbon input into soil from below-and aboveground litter in climatically contrasting forests. *Forest Ecology and Management*, *326*, 79–90. https://doi.org/10.1016/j.foreco.2014.03.039

Leppälammi-Kujansuu, J., Salemaa, M., Kleja, D. B., Linder, S., & Helmisaari, H.-S. (2014). Fine root turnover and litter production of Norway spruce in a long-term temperature and nutrient manipulation experiment. *Plant and Soil*, *374*(1), 73–88. https://doi.org/10.1007/s11104-013-1853-3

Leuschner, C., Hertel, D., Schmid, I., Koch, O., Muhs, A., & Hölscher, D. (2004). Stand fine root biomass and fine root morphology in old-growth beech forests as a function of precipitation and soil fertility. *Plant and Soil*, *258*(1), 43–56. https://doi.org/10.1023/B:PLSO.0000016508.20173.80

Liang, C., Schimel, J. P., & Jastrow, J. D. (2017). The importance of anabolism in microbial control over soil carbon storage. *Nature microbiology*, 2(8), 1-6.

Liang, X., Liu, S., Wang, H., & Wang, J. (2018). Variation of carbon and nitrogen stoichiometry along a chronosequence of natural temperate forest in northeastern China. *Journal of plant ecology*, 11(3), 339-350.

Lugato, E., Lavallee, J. M., Haddix, M. L., Panagos, P., & Cotrufo, M. F. (2021). Different climate sensitivity of particulate and mineral-associated soil organic matter. *Nature Geoscience*, *14*(5), Article 5. https://doi.org/10.1038/s41561-021-00744-x

Luo, Z., Wang, E., & Sun, O. J. (2016). A meta-analysis of the temporal dynamics of priming soil carbon decomposition by fresh carbon inputs across ecosystems. *Soil Biology and Biochemistry*, *101*, 96–103. https://doi.org/10.1016/j.soilbio.2016.07.011

Manzoni, S., & Porporato, A. (2009). Soil carbon and nitrogen mineralization: Theory and models across scales. *Soil Biology and Biochemistry*, *41*(7), 1355-1379.

Manzoni, S., Trofymow, J. A., Jackson, R. B., & Porporato, A. (2010). Stoichiometric controls on carbon, nitrogen, and phosphorus dynamics in decomposing litter. *Ecological monographs*, 80(1), 89-106.

Meier, I. C., & Leuschner, C. (2010). Variation of soil and biomass carbon pools in beech forests across a precipitation gradient. *Global Change Biology*, 16(3), 1035-1045.

Moyano, F. E., Manzoni, S., & Chenu, C. (2013). Responses of soil heterotrophic respiration to moisture availability: An exploration of processes and models. *Soil Biology and Biochem-istry*, 59, 72-85.

Parton, W. J., Hanson, P. J., Swanston, C., Torn, M., Trumbore, S. E., Riley, W., & Kelly, R. (2010). ForCent model development and testing using the Enriched Background Isotope Study experiment. *Journal of Geophysical Research: Biogeosciences*, *115*(G4). https://doi.org/10.1029/2009JG001193

Pei, G., Liu, J., Peng, B., Gao, D., Wang, C., Dai, W., Jiang, P., & Bai, E. (2019). Nitrogen, lignin, C/N as important regulators of gross nitrogen release and immobilization during litter decomposition in a temperate forest ecosystem. *Forest Ecology and Management*, *440*, 61–69. https://doi.org/10.1016/j.foreco.2019.03.001

Phillips, R. P., Finzi, A. C., & Bernhardt, E. S. (2011). Enhanced root exudation induces microbial feedbacks to N cycling in a pine forest under long-term CO2 fumigation. *Ecology Letters*, *14*(2), 187–194. https://doi.org/10.1111/j.1461-0248.2010.01570.x

Pietsch, K. A., Ogle, K., Cornelissen, J. H., Cornwell, W. K., Bönisch, G., Craine, J. M., … & Wirth, C. (2014). Global relationship of wood and leaf litter decomposability: the role of functional traits within and across plant organs. *Global Ecology and Biogeography*, 23(9), 1046-1057.

Rawls, W. J., Brakensiek, D. L., & Saxtonn, K. E. (1982). Estimation of soil water properties. *Transactions of the ASAE*, 25(5), 1316-1320.

Rousk, J., & Bååth, E. (2011). Growth of saprotrophic fungi and bacteria in soil. *FEMS Microbiology Ecology*, *78*(1), 17–30. https://doi.org/10.1111/j.1574-6941.2011.01106.x

Sato, A., & Seto, M. (1999). Relationship between rate of carbon dioxide evolution, microbial biomass carbon, and amount of dissolved organic carbon as affected by temperature and water content of a forest and an arable soil. *Communications in soil science and plant analysis*, 30(19-20), 2593-2605.

Schaufler, G., Kitzler, B., Schindlbacher, A., Skiba, U., Sutton. M.A., & Zechmeister-Boltenstern, S. (2010). Greenhouse gas emissions from European soils under different land use: effects of soil moisture and temperature. *European Journal of Soil Science*, 61, 683-696.

Scott, N. A., & Binkley, D. (1997). Foliage litter quality and annual net N mineralization: Comparison across North American forest sites. *Oecologia*, *111*(2), 151–159. https://doi.org/10.1007/s004420050219

Sinsabaugh, R. L., Manzoni, S., Moorhead, D. L., & Richter, A. (2013). Carbon use efficiency of microbial communities: Stoichiometry, methodology and modelling. *Ecology Letters*, 16(7), 930–939. *https://doi.org/10.1111/ele.12113*

Sinsabaugh, R. L., Turner, B. L., Talbot, J. M., Waring, B. G., Powers, J. S., Kuske, C. R., … & Follstad Shah, J. J. (2016). Stoichiometry of microbial carbon use efficiency in soils. *Ecological Monographs*, 86(2), 172-189.

Sinsabaugh, R. L., Shah, J. J. F., Findlay, S. G., Kuehn, K. A., & Moorhead, D. L. (2015). Scaling microbial biomass, metabolism and resource supply. *Biogeochemistry*, *122*(2), 175–190. *https://doi.org/10.1007/s10533-014-0058-z*

Stergiadi, M., van der Perk, M., de Nijs, T. C. M., & Bierkens, M. F. P. (2016). Effects of climate change and land management on soil organic carbon dynamics and carbon leaching in northwestern Europe. *Biogeosciences*, *13*(5), 1519–1536. https://doi.org/10.5194/bg-13-1519-2016.

Thimonier, A., Schmitt, M., Cherubini, P., & Kräuchi, N. (2001). Monitoring the Swiss forest: Building a research platform. *Monitoraggio Ambientale: Metodologie Ed Applicazioni. Atti Del XXXVIII Corso Di Cultura in Ecologia*, 121–134.

Tu, L., Hu, H., Chen, G., Peng, Y., Xiao, Y., Hu, T., Zhang, J., Li, X., Liu, L., & Tang, Y. (2014). Nitrogen Addition Significantly Affects Forest Litter Decomposition under High Levels of Ambient Nitrogen Deposition. *PLOS ONE*, *9*(2), e88752. https://doi.org/10.1371/journal.pone.0088752

Tückmantel, T., Leuschner, C., Preusser, S., Kandeler, E., Angst, G., Mueller, C. W., & Meier, I. C. (2017). Root exudation patterns in a beech forest: Dependence on soil depth, root morphology, and environment. *Soil Biology and Biochemistry*, *107*, 188–197. https://doi.org/10.1016/j.soilbio.2017.01.006

Templer, P. H., Mack, M. C., III, F. C., Christenson, L. M., Compton, J. E., Crook, H. D., … & Zak, D. R. (2012). Sinks for nitrogen inputs in terrestrial ecosystems: a meta-analysis of 15N tracer field studies. *Ecology*, 93(8), 1816-1829.

Wang, Q., Xiao, J., Ding, J., Zou, T., Zhang, Z., Liu, Q., & Yin, H. (2021). Differences in root exudate inputs and rhizosphere effects on soil N transformation between deciduous and evergreen trees. *Plant and Soil*, *458*(1), 277–289. https://doi.org/10.1007/s11104-019-04156-0

Weedon, J. T., Cornwell, W. K., Cornelissen, J. H. C., Zanne, A. E., Wirth, C., & Coomes, D. A. (2009). Global meta-analysis of wood decomposition rates: A role for trait variation among tree species? *Ecology Letters*, *12*(1), 45–56. https://doi.org/10.1111/j.1461-0248.2008.01259.x

Yuan, Z., & Chen, H. Y. H. (2009). Global trends in senesced-leaf nitrogen and phosphorus. *Global Ecology and Biogeography*, *18*(5), 532–542. https://doi.org/10.1111/j.1466-8238.2009.00474.x

Zagyvai-Kiss, K. A., Kalicz, P., Szilágyi, J., & Gribovszki, Z. (2019). On the specific water holding capacity of litter for three forest ecosystems in the eastern foothills of the Alps. *Agricultural and Forest Meteorology*, *278*, 107656.

Zhang, Q., Lei, H. M., & Yang, D. W. (2013). Seasonal variations in soil respiration, heterotrophic respiration and autotrophic respiration of a wheat and maize rotation cropland in the North China Plain. *Agricultural and Forest Meteorology*, 180, 34-43.

Zhang, X., & Wang, W. (2015). Control of climate and litter quality on leaf litter decomposition in different climatic zones. *Journal of Plant Research*, *128*(5), 791–802. https://doi.org/10.1007/s10265-015-0743-6

Zhang, Z., Qiao, M., Li, D., Yin, H., & Liu, Q. (2016). Do warming-induced changes in quantity and stoichiometry of root exudation promote soil N transformations via stimulation of soil nitrifiers, denitrifiers and ammonifiers? *European Journal of Soil Biology*, *74*, 60–68. https://doi.org/10.1016/j.ejsobi.2016.03.007